AFGL-TR-88-0321

AD-A205 276

Frequency Dependent Attenuation in Rocks

Karl B. Coyner
Randolph J. Martin

New England Research Inc
P.O. Box 857
Norwich, VT 05055

3 October 1988

Scientific Report No. 1

AIR FORCE GEOPHYSICS LABORATORY
AIR FORCE SYSTEMS COMMAND
UNITED STATES AIR FORCE
HANSCOM AIR FORCE BASE, MASSACHUSETTS 01731-5000

UNCLASSIFIED

SECURITY CLASSIFICATION OF THIS PAGE

REPORT DOCUMENTATION PAGE

Form Approved OMB No. 0704-0188

1a. REPORT SECURITY CLASSIFICATION: UNCLASSIFIED

1b. RESTRICTIVE MARKINGS:

2a. SECURITY CLASSIFICATION AUTHORITY:

2b. DECLASSIFICATION / DOWNGRADING SCHEDULE:

3. DISTRIBUTION / AVAILABILITY OF REPORT: Approved for Public Release; Distribution Unlimited

4. PERFORMING ORGANIZATION REPORT NUMBER(S):

5. MONITORING ORGANIZATION REPORT NUMBER(S): AFGL-TR-88-0321

6a. NAME OF PERFORMING ORGANIZATION: New England Research, Inc.

6b. OFFICE SYMBOL *(If applicable)***:**

7a. NAME OF MONITORING ORGANIZATION: Air Force Geophysics Laboratory

6c. ADDRESS *(City, State, and ZIP Code)***:** P.O. Box 857, Norwich, Vermont 05055

7b. ADDRESS *(City, State, and ZIP Code)***:** Hanscom AFB, MA 01731

8a. NAME OF FUNDING / SPONSORING ORGANIZATION: DARPA

8b. OFFICE SYMBOL *(If applicable)***:** NA

9. PROCUREMENT INSTRUMENT IDENTIFICATION NUMBER: F19628-87-C-0214

8c. ADDRESS *(City, State, and ZIP Code)***:** 1400 Wilson Boulevard, Arlington, VA 22209

10. SOURCE OF FUNDING NUMBERS

PROGRAM ELEMENT NO.	PROJECT NO.	TASK NO.	WORK UNIT ACCESSION NO.
62714E	7A10	DA	DA

11. TITLE *(Include Security Classification)* (U)

Frequency Dependent Attenuation In Rocks

12. PERSONAL AUTHOR(S): Karl B. Coyner, Randolph J. Martin

13a. TYPE OF REPORT	13b. TIME COVERED	14. DATE OF REPORT (Year, Month, Day)	15. PAGE COUNT
Scientific #1	FROM 9/2/87 TO 9/1/88	1988 October 3	26

16. SUPPLEMENTARY NOTATION:

17. COSATI CODES

FIELD	GROUP	SUB-GROUP

18. SUBJECT TERMS *(Continue on reverse if necessary and identify by block number)*

attenuation; anisotropy; rock properties; Stress strain relations; Granite; Laboratory tests. (edc)

19. ABSTRACT *(Continue on reverse if necessary and identify by block number)*

A comparison of laboratory Q values calculated from phase angles and hysteresis loop areas reveals an inconsistency. Q values calculated from hysteresis loops are a factor of 4 times greater than those from the phase angle. The source of this inconsistency is the definition of maximum strain energy for a hysteresis loop. An accounting of this factor of 4 is significant in comparing various experimental results that have ~~utilized~~ used either of the two techniques. Keywords; Seismic waves

20. DISTRIBUTION / AVAILABILITY OF ABSTRACT: ☒ UNCLASSIFIED/UNLIMITED ☐ SAME AS RPT. ☐ DTIC USERS

21. ABSTRACT SECURITY CLASSIFICATION: UNCLASSIFIED

22a. NAME OF RESPONSIBLE INDIVIDUAL	22b. TELEPHONE (Include Area Code)	22c. OFFICE SYMBOL
James F. Lewkowicz	617-377-3028	LWH

DD Form 1473, JUN 86 Previous editions are obsolete. SECURITY CLASSIFICATION OF THIS PAGE

UNCLASSIFIED

The Definition and Calculation of Q from Phase Angle and Hysteresis Loop Attenuation Measurements

Karl B. Coyner
New England Research, Inc.
P.O. Box 857, Norwich, Vermont 05055

Abstract. An inconsistency in the interpretation of experimental stress-strain data for Q determinations is investigated. Attenuation factors (Q^{-1}) calculated from the integrated areas of plotted hysteresis loops depend on the location of the origin for the hysteresis loop relative to the definition of maximum strain energy. This origin can be mislocated at one end of the hysteresis loop, as opposed to the center, resulting in Q^{-1} factors approximately a factor of 4 less than those calculated from the phase angle ϕ measured between cycled stress and strain ($Q^{-1}=\tan\phi$). Attenuation factors calculated from the ratio of hysteresis loop areas must be carefully interpreted before application to seismic wave propagation.

Introduction

The most seismologically relevant laboratory determinations of rock attenuation and moduli involve the direct measurement of stress-strain data with an applied periodic stress. Seismic frequencies between approximately 0.01 and 500 Hz and strain amplitudes between 10^{-7} and 10^{-3} have been attained with this technique. The material properties for evaluating high strain, nonlinear attenuation (Minster and Day, 1986), and the interpretation of the physical mechanisms of attenuation, particularly frequency dependence (Toksöz et al., 1987), must eventually rely on experimental data collected with this method. There is only a limited set of laboratory data available. Much of it is contradictory and often improperly interpreted.

Q factors may be calculated from either the phase angle ϕ between cycled stress and strain (Spencer, 1981; Jackson et al., 1984) or else from the hysteresis loops generated by

plotting the stress versus strain data (Gordon and Davis, 1968; Walsh et al., 1970; McKavanagh and Stacey, 1974; Brennan, 1981; Liu and Peselnick, 1983). A comparison has not been made between the two methods. Presumably, they should duplicate each other since the accepted equivalency is $Q^{-1} = \tan \phi = \delta W/2\pi W$, where δW is the amount of strain energy W dissipated during a cycle. The area of the hysteresis loop is proportional to δW and the area under the increasing load portion of the loop is proportional to W. Q values are calculated by integrating these respective areas of the hysteresis loop.

An examination of the two procedures indicates a potential inconsistency. Q values calculated from hystersis loops can be approximately four times greater than those from the phase angle. In the analysis section of this paper the source of this inconsistency is shown to be the definition of maximum strain energy and the relative location of the origin for zero stress and strain for the hysteresis loop. The accepted definition, from which the equivalency is derived, is appropriate for sinusoidal signals centered about zero stress and strain, i.e., a rock undergoing both compression and tension, for which the origin is at the center of the hysteresis loop. Maximum strain energy calculated for the compressive portion of the loop is approximately 1/4th of the overall peak to peak energy function.

Laboratory measurements, however, are normally biased by a pre-stress. If the origin is taken at the point of lowest stress and strain the measured value for maximum energy stored under the hysteresis loop is approximately a factor of 4 greater than the above definition. This results in a Q factor overestimated by a factor of 4. An accounting of this factor of 4 is significant in comparing various experimental results that have utilized either of the two techniques.

Hysteresis Loop Analysis

The time-varying stress $\sigma(t)$ and strain $\varepsilon(t)$ functions for a linear anelastic material deformed by a steady-state sinusoidal stress of frequency w and amplitude σ_0 is given by

$$\sigma(t)=\sigma_0 \sin(wt) \quad \text{and} \quad \varepsilon(t)=J\sigma_0 \sin(wt-\phi).$$

Since the material is anelastic the strain lags stress in time by the phase angle ϕ. The strain function may be expanded,

$$\varepsilon(t) = J_1 \sigma_0 \cos\phi \sin(wt) - J_2 \sigma_0 \sin\phi \cos(wt)$$

to yield "in-phase", sin(wt), and "out-of-phase", cos(wt), strain components of magnitude $J_1\sigma_0 = J\cos\phi\sigma_0$ and $J_2\sigma_0 = J\sin\phi\sigma_0$, respectively. The ratio of the components is $\tan\phi = J_2/J_1$. In the absence of anelasticity the linear stress-strain relationship is $\varepsilon = J\sigma$, where J is a compliance.

A plot of the stress-strain relationship described by these functions is an ellipse with the origin centered at zero stress and strain. This is often referred to as a hysteresis loop. In Fig. 1 is shown a hysteresis loop that was generated by introducing a phase angle of 0.0628 radians between two sine waves. The maximum and minimum stresses and strains are $\pm\sigma_0$ and $\pm J\sigma_0$, respectively, and the hysteresis loop is traced out in a clockwise direction.

The phase angle and the hysteresis loop are both equivalent expressions of the same anelastic process through which energy is absorbed. A dimensionless measure of anelasticity is the Q factor, which is an analogue of the Q used for characterizing the efficiency of voltage transfer in electric circuits. The inverse of Q may be called the attenuation factor (Q^{-1}), two expressions for which are

$$Q^{-1} = \tan\phi \quad \text{and} \quad Q^{-1} = \delta W/2\pi W.$$

The first expression is the "loss tangent" and refers to the tangent of the phase angle between stress and strain. In the second expression relative attenuation is obtained from the ratio of δW, the energy dissipated during one cycle, to the maximum strain energy W introduced into the sample during one cycle.

For the sinusoidal stress and strain time functions, representative of a linear anelastic material, the two definitions are equal. This can be easily shown by considering the hysteresis loop in Fig. 1. Stress times strain is strain energy, hence the areas within the hysteresis loop plot contain all of the necessary information for calculating the relative attenuation energy ratio. The maximum energy W supplied to the material is the shaded area of Fig. 1, corresponding to the

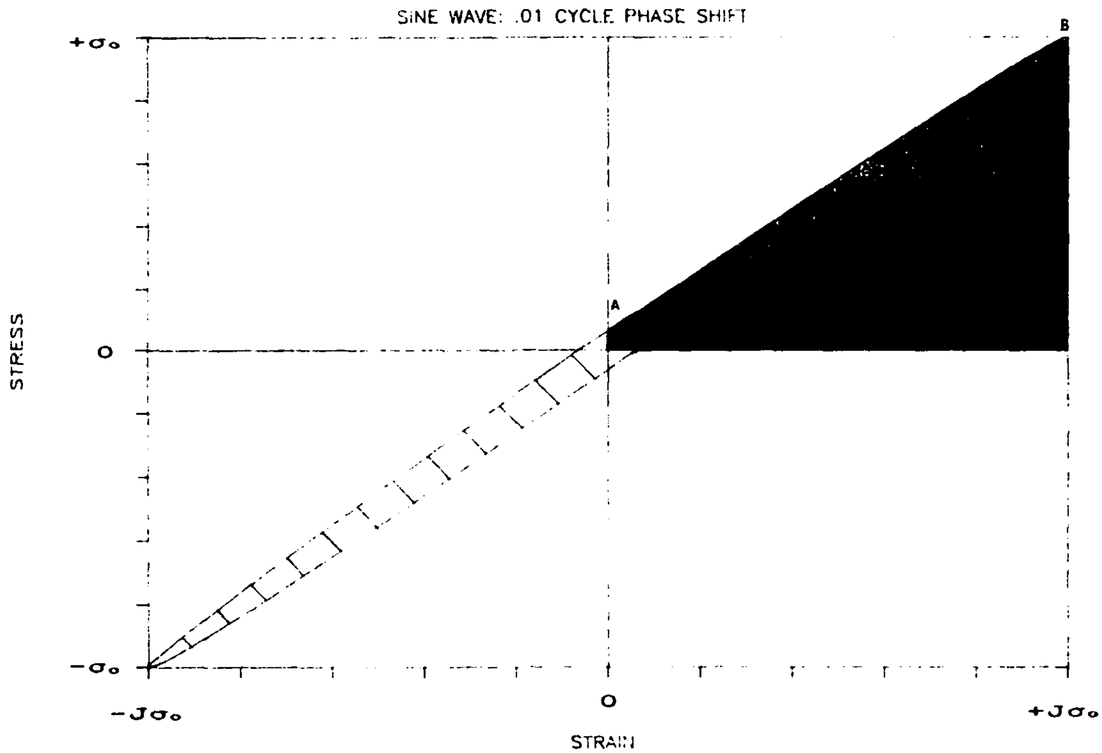

FIG. 1. Hysteresis loop derived from two sine waves offset by 0.01 cycles, or 0.0628 radians, centered at zero stress and strain. The shaded area is the maximum energy W introduced into a unit volume of sample during one cycle, corresponding to the path from A to B on the hysteresis loop. The interior area of the hysteresis loop δW is the energy dissipated per unit volume during one cycle. The attenuation factor is $Q^{-1} = \delta W/2\pi W = \tan(.0628)$.

deformation between points A and B, or the integral

$$W = \int_A^B \sigma \, d\varepsilon .$$

The dissipated energy δW is the cross-hatched area contained within the hysteresis loop, or the surface integral

$$\delta W = \oint \sigma \, d\varepsilon .$$

The integrals can be easily solved by noting from Fig. 1 that W is approximately the area of a triangle with sides σ_0 and $J\sigma_0$, and δW is the area of an ellipse with semimajor axis along the slope 1/J and semiminor axis along the slope -1/J. The lengths of the axes can be calculated from the intersections with the equation for the ellipse obtained from the stress-strain relation. The two integrals can therefore be geometrically computed for small attenuations as

$$W \approx \tfrac{1}{2} J_1 \sigma_0^2 \quad \text{and} \quad \delta W \approx \pi \tan\phi J_1 \sigma_0^2 .$$

Substituting for the ratio $W/\delta W$, it is found that

$$Q^{-1} = \delta W / 2\pi W = \tan \phi$$

and the definitions are thereby equivalent. For the hysteresis loop in Fig. 1, Q^{-1}=0.0629 (Q = 15.9).

For nonlinear materials and large attenuations the hysteresis loop becomes nonelliptical and nonsymmetrical, with cusped ends (McKavanagh and Stacey, 1974). In this instance it is necessary to integrate the areas of the hysteresis loop directly and to calculate the relative attenuation Q^{-1} from the energy ratio. The loss tangent or phase angle between stress and strain is not singularly defined.

Although the analysis of hysteresis loops is well-known (see, for example, Lorrain and Corson, 1970), an essential point is that the stress and strain functions are AC-signals, that is, centered about zero with equal positive and negative excursions and a hysteresis loop centered on the origin. Consequently, the maximum strain energy ($\approx \tfrac{1}{2} J\sigma_0^2$) is attained in only one-half of the overall peak-to-peak stress and strain amplitudes ($2\sigma_0$ and $2J\sigma_0$, respectively).

If the sinusoidal stress and strain time functions are DC-biased, i.e., offset so that they are continuously positive, the definitions of maximum strain energy W, relative attenuation ($Q^{-1}=\delta W/2\pi W$), and the identity of the hysteresis loop origin can become somewhat confusing. In Fig. 2 the same hysteresis loop as in Fig. 1 is replotted with the origin at zero stress and strain. The stress and strain time functions for this hysteresis loop have been shifted by $+\sigma_0$ and $+J\sigma_0$, although with the same peak-to-peak amplitudes of $2\sigma_0$ and $2J\sigma_0$. The energy dissipated during a cycle is still the area of the

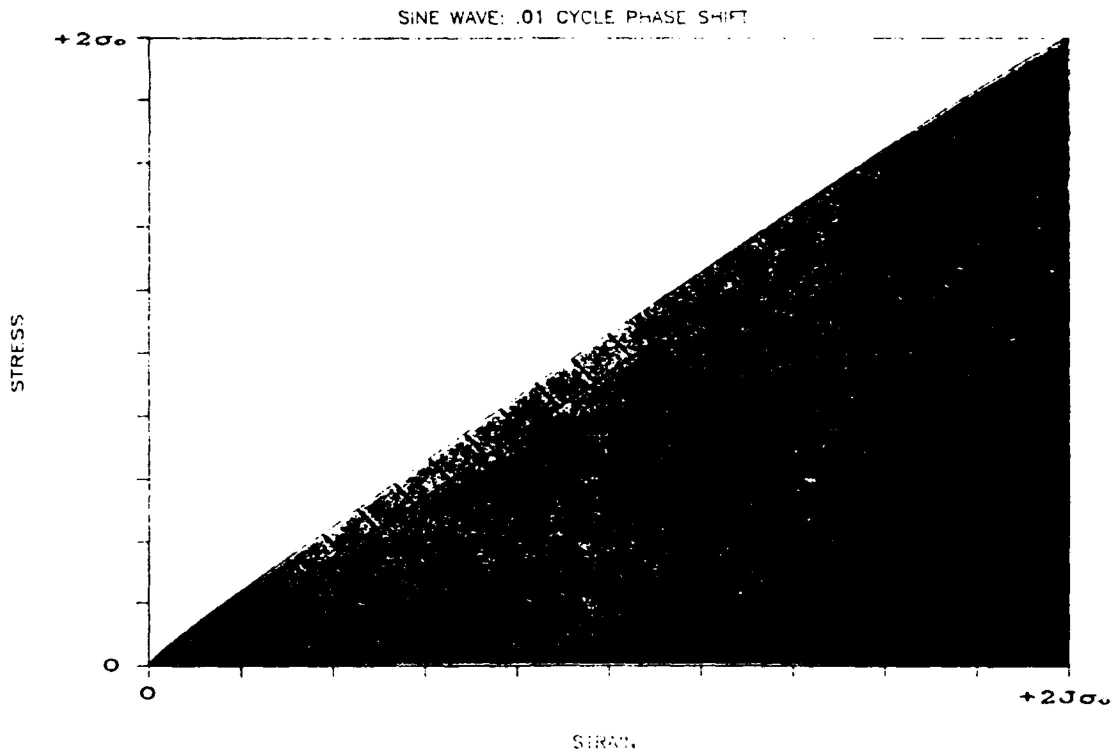

Fig. 2. Same hysteresis loop as in Fig. 1 but centered at $+\sigma_0$ stress and $+J\sigma_0$ strain. The shaded area is the maximum energy introduced per unit volume during the hysteresis loop cycle, but this gives an incorrect relative attenuation factor ($\frac{1}{4}Q^{-1}$) for the material at stress $+\sigma_0$ and $+J\sigma_0$ strain, for which this hysteresis loop is representative (see text).

ellipse, as in Fig. 1, or $\pi \tan\phi J_1 \sigma_0^2$. Maximum strain energy, however, or the shaded area under the loading portion of the hysteresis loop in Fig. 2, is

$$W \approx \tfrac{1}{2}\,(2\sigma_0)\,(2J_1\sigma_0) = 2J_1\sigma_0^2,$$

a factor of 4 times greater than before. Accordingly, when δW and W are substituted into the relative attenuation definition, the result is

$$Q^{-1} = \delta W/2\pi W = \tfrac{1}{4}\tan\phi.$$

Since the DC-bias has not changed the phase angle between stress and strain, the "loss-tangent" definition of attenuation

remains $Q^{-1} = \tan\phi$. The immediate and perplexing result is that the attenuation factor calculated from the hysteresis loop areas is 1/4th of that calculated from the tangent of the phase angle.

This apparent inconsistency can be resolved by re-examining the maximum strain energy W relative to the origin of the hysteresis loop in Fig. 2. From the external perspective of the sinusoidal stress driving the material the maximum strain energy is indeed $2J_1\sigma_0^2$. For the material, however, the state of stress and strain appropriate for the hysteresis loop and energy calculation is not at the origin of zero stress and strain in Fig. 2, but at the center of the hysteresis loop, i.e., as in Fig. 1. Although stress and strain are continuously positive, the material at $+\sigma_0$ stress and $+J\sigma_0$ strain is being cyclically deformed by stress and strain functions with amplitudes of $\pm\sigma_0$ and $\pm J\sigma_0$. Once this reference at the center of the hysteresis loop in Fig. 2 is adopted, the maximum strain energy is reduced to what it was for the hysteresis loop in Fig. 1, $\frac{1}{2}J_1\sigma_0^2$. The attenuation factors from the relative energy attenuation ratio and loss tangent then agree, $Q^{-1}=\delta W/2\pi W=\tan\phi$. This attenuation factor must be associated with the material at its stress and strain condition in the center of the hysteresis loop, $+\sigma_0$ and $+J\sigma_0$.

Discussion

Although the clarification of hysteresis loop analysis for Q determination is straightforward, the inconsistency in interpreting hysteresis loops has propagated through much of the available experimental stress-strain data available, particularly at high strain amplitudes. Therefore an accounting of this factor of 4 is significant, and tends to resolve at least one outstanding discrepancy while decreasing (by a factor of 4) typical Q's for rock at high strain amplitudes.

There are two techniques to measure and interpret attenuation from low-frequency stress-strain data. Either the phase angle is measured directly (Spencer, 1981; Jackson et al., 1984) or else the hysteresis loop is plotted out and the areas integrated (Gordon and Davis, 1968; Walsh et al., 1970; McKavanagh and Stacey, 1974; Brennan, 1981; Liu and Peselnick,

1983; Coyner, 1987). Hysteresis loop integration of the areas shown in Fig.2 and discussed in the analysis section leads to a relative attenuation Q factor that is greater than the loss tangent Q ($\tan\phi$) by a factor of 4. Therefore, in most instances the Q factors obtained by analyzing the areas of hysteresis loops have to be decreased by a factor of 4. This is particularly true if they are to be interpreted and compared with the Q factor results of other experimental techniques (field observations, resonant bar, ultrasonic).

In Table 1 is a tabulation of experimental Q factors from previous, low frequency, stress-strain results on room dry and vacuum dry rocks that were measured with either the phase angle or plotted hysteresis loop technique. The list of "reported" Q factors is collected from the respective references. The list of "corrected" values is suggested from the analysis results of this paper, i.e., reported Q's divided by a factor of 4. Only Spencer (1981) and Jackson et al. (1984) measured the phase angle directly and, consequently, their results do not require correction (References 5 and 7). For all of the others (Table 1) either the plotted hysteresis loops or a statement of procedure indicates that maximum strain energy was integrated under the entire loop, therebye resulting in an overestimation of Q by a factor of 4. Walsh et al. (1970), however, report their attenuation results as relative attenuation, $\delta W/W$, and not as Q factors. Nevertheless, in order to interpret the results as Q the relative attenuations still need to be divided by $4 * 2\pi$.

The strain amplitude dependence of attenuation changes quite dramatically if large strain amplitude Q factors are reduced by a factor of 4. Coyner (1987) found that hysteresis loop attenuation data at large strain amplitudes ($>10^{-4}$) was essentially equal to that from the ultrasonic pulse technique. After the correction by a factor of 4, however, the hysteresis loop attenuation factors are the largest (Q's the lowest). This is a far more plausible result, and indicates the significance of strain amplitude on attenuation.

At high strain amplitudes nonlinear friction dominates attenuation, and Q factors are extremely low, on the order of 2 to 50 (Table 1, references 1, 2, 3, and 8). In this group the Q factors for typical microcracked granites cluster in the range from 9 to 12.5 (references 1, 2, 8). The Q of 2 is for a friable, weathered, Cedar City diorite (Walsh et al., 1970).

TABLE 1. Reported and Corrected Hysteresis Loop Q Factors.

Rock (Dry)	Frequency (Hz)	Strain (10^{-6})	Q_E Reported	Q_F Corrected	Reference
Granite	.0005-.05	10^2-10^3	50	12.5	1
Quartzite	.0005-.05	10^2-10^3	200	50	1
Granite (Cedar City)	<.05	10^3-10^4	8-11	2-3	2
Granite (Westerly)	<.05	500	45	11	2
Granite, basalt, and sandstone	.003-.1	1-10	100	25	3
Basalt	.001-.5	1.7	525 (Q_S)	130	4
Granite	.001-.5	1.1	266 (Q_S)	67	4
Sandstone	.001-.5	1.2	75-125(Q_S)	19-31	4
Sandstone, granite, limestone (vacuum dry)	.004-.4	0.1	>500	>500	5
Granite (Westerly)	.01-1	.01-.1	>450	>112.5	6
Granite (P_c >10 MPa)	.33-.003	0.6	400-2000(Q_S)	400-2000	7
Granite (Sierra White)	0.1	10-10^3	36-50	9-12	8

References: 1, Gordon and Davis, 1968; 2, Walsh et al., 1970; 3, McKavanagh and Stacey, 1974; 4, Brennan, 1981; 5, Spencer, 1981; 6, Liu and Peselnick, 1983; 7, Jackson et al., 1984; 8, Coyner, 1987.

One discrepancy that is resolved when hysteresis loop Q factors are reduced by a factor of 4 is the convergence of Q data of Liu and Peselnick (1983) compared to that of Spencer (1981). Both experimentally measured low frequency, low strain amplitude (<10^{-6} strain), stress-strain data on cylinders of granite sinusoidally loaded at low pressure. A major concern with the results of Liu and Peselnick, however, is a large Q (>450) for room dry Westerly granite. This is a saturation condition that contrasts with the large Q (>500) observed by Spencer for vacuum dry Oklahoma granite.

These similar results seem unusual since the work of Tittmann (1973) and Clark et al. (1980) has underscored the substantial decrease in Q caused by the presence of volatiles, particularly water. Resonant bar measurements by Coyner (1987) on room dry Sierra White granite found Q factors of approximately 125, similar to those found by Winkler et al. (1979) for Sierra White and Tittmann (1984) for Westerly granite. Therefore the Liu and Peselnick data point appears anomalous because the Q factor is so high for a room-dry rock at zero confining pressure. If the hysteresis loop data of Liu and Peselnick are re-interpreted, and the Q factor decreased by a factor of 4, to Q>112, the room condition Q's for granite all fall within the same range (Q's from 67 to 125). (It must be noted, however, that several different granites are involved, and Liu and Peselnick do not show any plots of hysteresis loops.) Large Q's for typical microcracked granite are therefore preserved for vaccuum conditions (Spencer, 1981) or samples under confining pressure (Jackson et al., 1984).

Although modern experimental technique and digital signal analysis favors the direct measurement of phase angle in these experiments, the hysteresis loop shape is still necessary for correct interpretation of linear behavior, i.e., elliptical versus cusped hysteresis loops. Brennan and Stacey (1977) measured the transition of loops from cusped to elliptical shapes as the strain amplitude fell to around 10^{-6} but do not show any plots of loop data. It seems reasonable to expect that hysteresis loops should be plotted in tandem with phase angles. The lack of this information makes it difficult to assess exactly how the attenuation from hysteresis loops has been calculated, and fails to document the hysteresis loop shape, which contains information on the nature of frictional attenuation.

Conclusions

It has been shown that direct stress-strain calculations of attenuation can lead to inconsistent results when comparing phase angle with hysteresis loop measurements. Quality factors (Q's) derived from the areas of hysteresis loops must be multiplied by a factor of 4 in order to be comparable to those from the phase angle, if the maximum strain energy is taken as the entire area under the loading portion of the hysteresis loop. Previous experimental data must be interpreted and compared in light of this correction factor. In particular, the strain amplitude dependence of Q is greater than previously realized, and room dry granite can have Q's as low as 2 to 30 at amplitudes greater than 10 microstrain.

REFERENCES

Brennan, B.J., and F.D. Stacey, Frequency dependence of elasticity of rock-test of seismic velocity dispersion, Nature, 268, 220-222, 1977.

Brennan, B.J., Linear viscoelastic behavior in rocks, in Anelasticity in the Earth, Geodyn. Ser., vol. 4, edited by F.D. Stacey, M.S. Paterson, and A. Nicolas, pp. 13-22, AGU, Washington, D.C., 1981.

Clark, V.A., B.R. Tittmann, and T.W. Spencer, Effect of volatiles on attenuation (Q^{-1}) and velocity in sedimentary rocks, J. Geophys. Res., 85, 5190-5198, 1980.

Coyner, K.B., 1987, Attenuation measurements on dry Sierra White granite, dome salt, and Berea sandstone, final report to Lawrence Livermore National Laboratory, Contract #9092405.

Gordon, R.B., and L.A. Davis, Velocity and attenuation of seismic waves in imperfectly elastic rock, J. Geophys. Res., 73, 3917-3935, 1968.

Jackson, I., M.S. Paterson, H. Niesler, and R.M. Waterford, Rock anelasticity measurements at high pressure, low strain amplitude and seismic frequency, Geophysical Research Letters, 11, 1235-1238, 1984.

Liu, H.-P., and L. Peselnick, Investigation of internal friction in fused quartz, steel, plexiglass, and Westerly granite from 0.01 to 1.00 Hertz at 10^{-8} to 10^{-7} strain amplitude, J. Geophys. Res., 88, 2367-2379, 1983.

McKavanagh, B., and F.D. Stacey, Mechanical hysteresis in rocks at low strain amplitudes and seismic frequencies, Physics of the Earth and Planetary Interiors, 8, 246-250, 1974.

Minster, J.B., and S.M. Day, Decay of wave fields near an explosive source due to high-strain, nonlinear attenuation, Journal of Geophysical Research, 91, 2113-2122, 1986.

Spencer, J.W., Stress relaxations at low frequencies in fluid-saturated rocks: Attenuation and modulus dispersion, J. Geophys. Res., 86, 1803-1812, 1981.

Tittmann, B.R., Internal friction measurements and their implications in seismic Q structure models of the crust, in The Earth's Crust: Monograph 20, AGU, 197-213, 1977.

Tittmann, B.R., Nonlinear wave propagation study, semi-annual technical report No. 2 for the period December 1, 1983 through May 31, 1984, SC5361.6SAR, Rockwell International Science Center, 1984.

Toksöz, M.N., E. Reiter, and B. Mandal, 1988, Seismic attenuation in the crust, Proc. 10th Ann. DARPA/AFGL Res. Symp., 127-134.

Walsh, J.B., Seismic wave attenuation in rock due to friction, J. Geophys. Res., 71, 2591-2599, 1966.

Walsh, J.B., W.F. Brace, and W.R. Wawersik, Attenuation of stress waves in Cedar City quartz diorite, Technical Report No. AFWL-TR-70-8, M.I.T., 1970.

Winkler, K.W., A. Nur, and M. Gladwin, Friction and seismic attenuation in rocks, Nature, 277, 528-531, 1979.

Professor Keiiti Aki
Center for Earth Sciences
University of Southern California
University Park
Los Angeles, CA 90089-0741

Professor Charles B. Archambeau
Cooperative Institute for Resch
in Environmental Sciences
University of Colorado
Boulder, CO 80309

Dr. Thomas C. Bache Jr.
Science Applications Int'l Corp.
10210 Campus Point Drive
San Diego, CA 92121 (2 copies)

Dr. Douglas R. Baumgardt
Signal Analysis & Systems Div.
ENSCO, Inc.
5400 Port Royal Road
Springfield, VA 22151-2388

Dr. Jonathan Berger
Institute of Geophysics and
Planetary Physics
Scripps Institution of Oceanography
A-025
University of California, San Diego
La Jolla, CA 92093

Dr. S. Bratt
Science Applications Int'l Corp.
10210 Campus Point Drive
San Diego, CA 92121

Dr. Lawrence J. Burdick
Woodward-Clyde Consultants
P.O. Box 93245
Pasadena, CA 91109-3245 (2 copies)

Professor Robert W. Clayton
Seismological Laboratory/Div. of
Geological & Planetary Sciences
California Institute of Technology
Pasadena, CA 91125

Dr Karl Coyner
N. E. Research
P.O. Box 857
Norwich, VT 05055

Dr. Vernon F. Cormier
Department of Geology & Geophysics
U-45, Roon 207
The University of Conneticut
Storrs, Connecticut 06268

Dr. Steven Day
Dept. of Geological Sciences
San Diego State U.
San Diego, CA 92182

Dr. Zoltan A. Der
ENSCO, Inc.
5400 Port Royal Road
Springfield, VA 22151-2388

Professor John Ferguson
Center for Lithospheric Studies
The University of Texas at Dallas
P.O. Box 830688
Richardson, TX 75083-0688

Professor Stanley Flatte'
Applied Sciences Building
University of California,
Santa Cruz, CA 95064

Dr. Alexander Florence
SRI International
333 Ravenswood Avenue
Menlo Park, CA 94025-3493

Professor Steven Grand
Department of Geology
245 Natural History Building
1301 West Green Street
Urbana, IL 61801

Dr. Henry L. Gray
Associate Dean of Dedman College
Department of Statistical Sciences
Southern Methodist University
Dallas, TX 75275

Professor Roy Greenfield
Geosciences Department
403 Deike Building
The Pennsylvania State University
University Park, PA 16802

Professor David G. Harkrider
Seismological Laboratory
Div of Geological & Planetary Sciences
California Institute of Technology
Pasadena, CA 91125

Professor Donald V. Helmberger
Seismological Laboratory
Div of Geological & Planetary Sciences
California Institute of Technology
Pasadena, CA 91125

Professor Eugene Herrin
Institute for the Study of Earth
& Man/Geophysical Laboratory
Southern Methodist University
Dallas, TX 75275

Professor Robert B. Herrmann
Department of Earth & Atmospheric
Sciences
Saint Louis University
Saint Louis, MO 63156

Professor Bryan Isacks
Cornell University
Dept of Geological Sciences
SNEE Hall
Ithaca, NY 14850

Professor Lane R. Johnson
Seismographic Station
University of California
Berkeley, CA 94720

Professor Thomas H. Jordan
Department of Earth, Atmospheric
and Planetary Sciences
Mass Institute of Technology
Cambridge, MA 02139

Dr. Alan Kafka
Department of Geology &
Geophysics
Boston College
Chestnut Hill, MA 02167

Professor Leon Knopoff
University of California
Institute of Geophysics
& Planetary Physics
Los Angeles, CA 90024

Professor Charles A. Langston
Geosciences Department
403 Deike Building
The Pennsylvania State University
University Park, PA 16802

Professor Thorne Lay
Department of Geological Sciences
1006 C.C. Little Building
University of Michigan
Ann Harbor, MI 48109-1063

Dr. Randolph Martin III
New England Research, Inc.
P.O. Box 857
Norwich, VT 05055

Dr. Gary McCartor
Mission Research Corp.
735 State Street
P.O. Drawer 719
Santa Barbara, CA 93102 (2 copies)

Professor Thomas V. McEvilly
Seismographic Station
University of California
Berkeley, CA 94720

Dr. Keith L. McLaughlin
S-CUBED,
A Division of Maxwell Laboratory
P.O. Box 1620
La Jolla, CA 92038-1620

Professor William Menke
Lamont-Doherty Geological Observatory
of Columbia University
Palisades, NY 10964

Professor Brian J. Mitchell
Department of Earth & Atmospheric
Sciences
Saint Louis University
Saint Louis, MO 63156

Mr. Jack Murphy
S-CUBED
A Division of Maxwell Laboratory
11800 Sunrise Valley Drive
Suite 1212
Reston, VA 22091 (2 copies)

Professor J. A. Orcutt
Institute of Geophysics and Planetary
Physics, A-205
Scripps Institute of Oceanography
Univ. of California, San Diego
La Jolla, CA 92093

Professor Keith Priestley
University of Nevada
Mackay School of Mines
Reno, NV 89557

Professor Paul G. Richards
Lamont-Doherty Geological
Observatory of Columbia Univ.
Palisades, NY 10964

Wilmer Rivers
Teledyne Geotech
314 Montgomery Street
Alexandria, VA 22314

Dr. Alan S. Ryall, Jr.
Center of Seismic Studies
1300 North 17th Street
Suite 1450
Arlington, VA 22209-2308 (4 copies)

Professor Charles G. Sammis
Center for Earth Sciences
University of Southern California
University Park
Los Angeles, CA 90089-0741

Professor Christopher H. Scholz
Geological Sciences
Lamont-Doherty Geological Observatory
Palisades, NY 10964

Dr. Jeffrey L. Stevens
S-CUBED,
A Division of Maxwell Laboratory
P.O. Box 1620
La Jolla, CA 92038-1620

Professor Brian Stump
Institute for the Study of Earth & Man
Geophysical Laboratory
Southern Methodist University
Dallas, TX 75275

Professor Ta-liang Teng
Center for Earth Sciences
University of Southern California
University Park
Los Angeles, CA 90089-0741

Dr. Clifford Thurber
State University of New York at
Stony Brooks
Dept of Earth and Space Sciences
Stony Brook, NY 11794-2100

Professor M. Nafi Toksoz
Earth Resources Lab
Dept of Earth, Atmospheric and
Planetary Sciences
Massachusetts Institute of Technology
42 Carleton Street
Cambridge, MA 02142

Professor Terry C. Wallace
Department of Geosciences
Building #11
University of Arizona
Tucson, AZ 85721

Weidlinger Associates
ATTN: Dr. Gregory Wojcik
4410 El Camino Real, Suite 110
Los Altos, CA 94022

Professor Francis T. Wu
Department of Geological Sciences
State University of New York
at Binghamton
Vestal, NY 13901

<u>OTHERS (United States)</u>

Dr. Monem Abdel-Gawad
Rockwell Internat'l Science Center
1049 Camino Dos Rios
Thousand Oaks, CA 91360

Professor Shelton S. Alexander
Geosciences Department
403 Deike Building
The Pennsylvania State University
University Park, PA 16802

Dr. Ralph Archuleta
Department of Geological
Sciences
Univ. of California at
Santa Barbara
Santa Barbara, CA

Dr. Muawia Barazangi
Geological Sciences
Cornell University
Ithaca, NY 14853

J. Barker
Department of Geological Sciences
State University of New York
at Binghamton
Vestal, NY 13901

Mr. William J. Best
907 Westwood Drive
Vienna, VA 22180

Dr. N. Biswas
Geophysical Institute
University of Alaska
Fairbanks, AK 99701

Dr. G. A. Bollinger
Department of Geological Sciences
Virginia Polytechnical Institute
21044 Derring Hall
Blacksburg, VA 24061

Dr. James Bulau
Rockwell Int'l Science Center
1049 Camino Dos Rios
P.O. Box 1085
Thousand Oaks, CA 91360

Mr. Roy Burger
1221 Serry Rd.
Schenectady, NY 12309

Dr. Robert Burridge
Schlumberger-Doll Resch Ctr.
Old Quarry Road
Ridgefield, CT 06877

Science Horizons, Inc.
ATTN: Dr. Theodore Cherry
710 Encinitas Blvd., Suite 101
Encinitas, CA 92024 (2 copies)

Professor Jon F. Claerbout
Professor Amos Nur
Dept. of Geophysics
Stanford University
Stanford, CA 94305 (2 copies)

Dr. Anton W. Dainty
AFGL/LWH
Hanscom AFB, MA 01731

Professor Adam Dziewonski
Hoffman Laboratory
Harvard University
20 Oxford St.
Cambridge, MA 02138

Professor John Ebel
Dept of Geology & Geophysics
Boston College
Chestnut Hill, MA 02167

Dr. Donald Forsyth
Dept. of Geological Sciences
Brown University
Providence, RI 02912

Dr. Anthony Gangi
Texas A&M University
Department of Geophysics
College Station, TX 77843

Dr. Freeman Gilbert
Institute of Geophysics &
Planetary Physics
Univ. of California, San Diego
P.O. Box 109
La Jolla, CA 92037

Mr. Edward Giller
Pacific Seirra Research Corp.
1401 Wilson Boulevard
Arlington, VA 22209

Dr. Jeffrey W. Given
Sierra Geophysics
11255 Kirkland Way
Kirkland, WA 98033

Rong Song Jih
Teledyne Geotech
314 Montgomery Street
Alexandria, Virginia 22314

Professor F.K. Lamb
University of Illinois at
Urbana-Champaign
Department of Physics
1110 West Green Street
Urbana, IL 61801

Dr. Arthur Lerner-Lam
Lamont-Doherty Geological Observatory
of Columbia University
Palisades, NY 10964

Dr. L. Timothy Long
School of Geophysical Sciences
Georgia Institute of Technology
Atlanta, GA 30332

Dr. Peter Malin
University of California at Santa Barbara
Institute for Central Studies
Santa Barbara, CA 93106

Dr. George R. Mellman
Sierra Geophysics
11255 Kirkland Way
Kirkland, WA 98033

Dr. Bernard Minster
Institute of Geophysics and Planetary
Physics, A-205
Scripps Institute of Oceanography
Univ. of California, San Diego
La Jolla, CA 92093

Professor John Nabelek
College of Oceanography
Oregon State University
Corvallis, OR 97331

Dr. Geza Nagy
U. California, San Diego
Dept of Ames, M.S. B-010
La Jolla, CA 92093

Dr. Jack Oliver
Department of Geology
Cornell University
Ithaca, NY 14850

Dr. Robert Phinney/Dr. F.A. Dahlen
Dept of Geological
Geophysical Sci. University
Princeton University
Princeton, NJ 08540 (2 copies)

RADIX Systems, Inc.
Attn: Dr. Jay Pulli
2 Taft Court, Suite 203
Rockville, Maryland 20850

Dr. Norton Rimer
S-CUBED
A Division of Maxwell Laboratory
P.O. 1620
La Jolla, CA 92038-1620

Professor Larry J. Ruff
Department of Geological Sciences
1006 C.C. Little Building
University of Michigan
Ann Arbor, MI 48109-1063

Dr. Richard Sailor
TASC Inc.
55 Walkers Brook Drive
Reading, MA 01867

Thomas J. Sereno, Jr.
Service Application Int'l Corp.
10210 Campus Point Drive
San Diego, CA 92121

Dr. David G. Simpson
Lamont-Doherty Geological Observ.
of Columbia University
Palisades, NY 10964

Dr. Bob Smith
Department of Geophysics
University of Utah
1400 East 2nd South
Salt Lake City, UT 84112

Dr. S. W. Smith
Geophysics Program
University of Washington
Seattle, WA 98195

Dr. Stewart Smith
IRIS Inc.
1616 N. Fort Myer Drive
Suite 1440
Arlington, VA 22209

Rondout Associates
ATTN: Dr. George Sutton,
Dr. Jerry Carter, Dr. Paul Pomeroy
P.O. Box 224
Stone Ridge, NY 12484 (4 copies)

Dr. L. Sykes
Lamont Doherty Geological Observ.
Columbia University
Palisades, NY 10964

Dr. Pradeep Talwani
Department of Geological Sciences
University of South Carolina
Columbia, SC 29208

Dr. R. B. Tittmann
Rockwell International Science Center
1049 Camino Dos Rios
P.O. Box 1085
Thousand Oaks, CA 91360

Professor John H. Woodhouse
Hoffman Laboratory
Harvard University
20 Oxford St.
Cambridge, MA 02138

Dr. Gregory B. Young
ENSCO, Inc.
5400 Port Royal Road
Springfield, VA 22151-2388

OTHERS (FOREIGN)

Dr. Peter Basham
Earth Physics Branch
Geological Survey of Canada
1 Observatory Crescent
Ottawa, Ontario
CANADA K1A OY3

Dr. Eduard Berg
Institute of Geophysics
University of Hawaii
Honolulu, HI 96822

Dr. Michel Bouchon - Universite
Scientifique et Medicale de Grenob
Lab de Geophysique - Interne et
Tectonophysique - I.R.I.G.M-B.P.
38402 St. Martin D'Heres
Cedex FRANCE

Dr. Hilmar Bungum/NTNF/NORSAR
P.O. Box 51
Norwegian Council of Science,
Industry and Research, NORSAR
N-2007 Kjeller, NORWAY

Dr. Michel Campillo
I.R.I.G.M.-B.P. 68
38402 St. Martin D'Heres
Cedex, FRANCE

Dr. Kin-Yip Chun
Geophysics Division
Physics Department
University of Toronto
Ontario, CANADA M5S 1A7

Dr. Alan Douglas
Ministry of Defense
Blacknest, Brimpton,
Reading RG7-4RS
UNITED KINGDOM

Dr. Manfred Henger
Fed. Inst. For Geosciences & Nat'l Res.
Postfach 510153
D-3000 Hannover 51
FEDERAL REPUBLIC OF GERMANY

Dr. E. Husebye
NTNF/NORSAR
P.O. Box 51
N-2007 Kjeller, NORWAY

Ms. Eva Jonannisson
Senior Research Officer
National Defense Research Inst.
P.O. Box 27322
S-102 54 Stockholm
SWEDEN

Tormod Kvaerna
NTNF/NORSAR
P.O. Box 51
N-2007 Kjeller, NORWAY

Mr. Peter Marshall, Procurement
Executive, Ministry of Defense
Blacknest, Brimpton,
Reading FG7-4RS
UNITED KINGDOM (3 copies)

Dr. Ben Menaheim
Weizman Institute of Science
Rehovot, ISRAEL 951729

Dr. Svein Mykkeltveit
NTNF/NORSAR
P.O. Box 51
N-2007 Kjeller, NORWAY (3 copies)

Dr. Robert North
Geophysics Division
Geological Survey of Canada
1 Observatory crescent
Ottawa, Ontario
CANADA, K1A OY3

Dr. Frode Ringdal
NTNF/NORSAR
P.O. Box 51
N-2007 Kjeller, NORWAY

Dr. Jorg Schlittenhardt
Federal Inst. for Geosciences & Nat'l Res.
Postfach 510153
D-3000 Hannover 51
FEDERAL REPUBLIC OF GERMANY

University of Hawaii
Institute of Geophysics
ATTN: Dr. Daniel Walker
Honolulu, HI 96822

FOREIGN CONTRACTORS

Dr. Ramon Cabre, S.J.
c/o Mr. Ralph Buck
Economic Consular
American Embassy
APO Miami, Florida 34032

Professor Peter Harjes
Institute for Geophysik
Rhur University/Bochum
P.O. Box 102148, 4630 Bochum 1
FEDERAL REPUBLIC OF GERMANY

Professor Brian L.N. Kennett
Research School of Earth Sciences
Institute of Advanced Studies
G.P.O. Box 4
Canberra 2601
AUSTRALIA

Dr. B. Massinon
Societe Radiomana
27, Rue Claude Bernard
7,005, Paris, FRANCE (2 copies)

Dr. Pierre Mechler
Societe Radiomana
27, Rue Claude Bernard
75005, Paris, FRANCE

GOVERNMENT

Dr. Ralph Alewine III
DARPA/NMRO
1400 Wilson Boulevard
Arlington, VA 22209-2308

Dr. Robert Blandford
DARPA/NMRO
1400 Wilson Boulevard
Arlington, VA 22209-2308

Sandia National Laboratory
ATTN: Dr. H. B. Durham
Albuquerque, NM 87185

Dr. Jack Evernden
USGS-Earthquake Studies
345 Middlefield Road
Menlo Park, CA 94025

U.S. Geological Survey
ATTN: Dr. T. Hanks
Nat'l Earthquake Resch Center
345 Middlefield Road
Menlo Park, CA 94025

Dr. James Hannon
Lawrence Livermore Nat'l Lab.
P.O. Box 808
Livermore, CA 94550

Paul Johnson
ESS-4, Mail Stop J979
Los Alamos National Laboratory
Los Alamos, NM 87545

Ms. Ann Kerr
DARPA/NMRO
1400 Wilson Boulevard
Arlington, VA 22209-2308

Dr. Max Koontz
US Dept of Energy/DP 5
Forrestal Building
1000 Independence Ave.
Washington, D.C. 20585

Dr. W. H. K. Lee
USGS
Office of Earthquakes, Volcanoes,
& Engineering
Branch of Seismology
345 Middlefield Rd
Menlo Park, CA 94025

Dr. William Leith
USGS
Mail Stop 928
Reston, VA 22092

Dr. Richard Lewis
Dir. Earthquake Engineering and
Geophysics
U.S. Army Corps of Engineers
Box 631
Vicksburg, MS 39180

Dr. Robert Masse'
Box 25046, Mail Stop 967
Denver Federal Center
Denver, Colorado 80225

Richard Morrow
ACDA/VI
Room 5741
320 21st Street N.W.
Washington, D.C. 20451

Dr. Keith K. Nakanishi
Lawrence Livermore National Laboratory
P.O. Box 808, L-205
Livermore, CA 94550 (2 copies)

Dr. Carl Newton
Los Alamos National Lab.
P.O. Box 1663
Mail Stop C335, Group E553
Los Alamos, NM 87545

Dr. Kenneth H. Olsen
Los Alamos Scientific Lab.
Post Office Box 1663
Los Alamos, NM 87545

Howard J. Patton
Lawrence Livermore National
Laboratory
P.O. Box 808, L-205
Livermore, CA 94550

Mr. Chris Paine
Office of Senator Kennedy
SR 315
United States Senate
Washington, D.C. 20510

AFOSR/NP
ATTN: Colonel Jerry J. Perrizo
Bldg 410
Bolling AFB, Wash D.C. 20332-6448

HQ AFTAC/TT
Attn: Dr. Frank F. Pilotte
Patrick AFB, Florida 32925-6001

Mr. Jack Rachlin
USGS - Geology, Rm 3 C136
Mail Stop 928 National Center
Reston, VA 22092

Robert Reinke
AFWL/NTESG
Kirtland AFB, NM 87117-6008

HQ AFTAC/TGR
Attn: Dr. George H. Rothe
Patrick AFB, Florida 32925-6001

Donald L. Springer
Lawrence Livermore National Laboratory
P.O. Box 808, L-205
Livermore, CA 94550

Dr. Lawrence Turnbull
OSWR/NED
Central Intelligence Agency
CIA, Room 5G48
Washington, D.C. 20505

Dr. Thomas Weaver
Los Alamos Scientific Laboratory
Los Almos, NM 97544

AFGL/SULL
Research Library
Hanscom AFB, MA 01731-5000 (2 copies)

Secretary of the Air Force (SAFRD)
Washington, DC 20330
Office of the Secretary Defense
DDR & E
Washington, DC 20330

HQ DNA
ATTN: Technical Library
Washington, DC 20305

DARPA/RMO/RETRIEVAL
1400 Wilson Blvd.
Arlington, VA 22209

DARPA/RMO/Security Office
1400 Wilson Blvd.
Arlington, VA 22209

AFGL/XO
Hanscom AFB, MA 01731-5000

AFGL/LW
Hanscom AFB, MA 01731-5000

DARPA/PM
1400 Wilson Boulevard
Arlington, VA 22209

Defense Technical
Information Center
Cameron Station
Alexandria, VA 22314
(5 copies)

Defense Intelligence Agency
Directorate for Scientific &
Technical Intelligence
Washington, D.C. 20301

Defense Nuclear Agency/SPSS
ATTN: Dr. Michael Shore
6801 Telegraph Road
Alexandria, VA 22310

AFTAC/CA (STINFO)
Patrick AFB, FL 32925-6001

Dr. Gregory van der Vink
Congress of the United States
Office of Technology Assessment
Washington, D.C. 20510

Mr. Alfred Lieberman
ACDA/VI-OA'State Department Building
Room 5726
320 - 21St Street, NW
Washington, D.C. 20451

TACTEC
Battelle Memorial Institute
505 King Avenue
Columbus, OH 43201 (Final report only)